Optical, Thermal, and Mechanical Characterization of Ga_2Se_3-Added GLS Glass

Andrea Ravagli, Christopher Craig, Ghada A. Alzaidy, Paul Bastock, and Daniel W. Hewak*

Gallium lanthanum sulfide glass (GLS) has been widely studied in the last 40 years for middle-infrared applications. In this work, the results of the substitution of selenium for sulphur in GLS glass are described. The samples are prepared via melt-quench method in an argon-purged atmosphere. A wide range of compositional substitutions are studied to define the glass-forming region of the modified material. The complete substitution of Ga_2S_3 by Ga_2Se_3 is achieved by involving new higher quenching rate techniques compared to those containing only sulfides. The samples exhibiting glassy characteristics are further characterized. In particular, the optical and thermal properties of the sample are investigated in order to understand the role of selenium in the formation of the glass. The addition of selenium to GLS glass generally results in a lower glass transition temperature and an extended transmission window. Particularly, the IR edge is found to be extended from about 9 µm for GLS glass to about 15 µm for Se-added GLS glass defined by the 50% transmission point. Furthermore, the addition of selenium does not affect the UV edge dramatically. The role of selenium is hypothesized in the glass formation to explain these changes.

Chalcogenide glasses are amorphous materials consisting of chalcogen elements (S, Se, Te) bonded with metals and semiconductors. The covalent bond between chalcogens and other elements gives exceptional properties to these materials.[1] The high atomic weight of the constituent atoms influences the low energy bandgap and transparency in the infrared (IR) with transmission up to 13 µm for sulfide glasses, 17 µm for selenide glasses, and 20 µm for telluride glasses.[2] The high content of heavy elements also results in glasses that are very dense, with high linear refractive index (n = 2–3) and pronounced nonlinear effects.[1,3,4]

Gallium lanthanum sulfide (GLS) glasses have received much attention for active applications in IR optics and photonics. Their constituent heavy elements lead to low frequency phonons which make chalcogenides suitable as rare earth hosts with decreased nonradiative decay opening up several transitions in the infrared not seen in traditional oxide glasses.[1,5–9]

A. Ravagli, C. Craig, G. A. Alzaidy, Dr. P. Bastock, Prof. D. W. Hewak
Optoelectronics Research Centre
University of Southampton
Salisbury Road, SO17 1BJ Southampton, UK
E-mail: ar1e15@soton.ac.uk

DOI: 10.1002/adma.201606329

The aim of this work is to improve the infrared transmission range without compromising the transmission in the visible range and other properties. Transparent glasses in both the visible and key thermal windows, around 3–8 µm (middle-infrared, MIR) and 8–15 µm longwave infrared (LWIR) radiation range, are currently required for multispectral imagining. Such materials can simplify the design of cameras that currently rely on several discrete optical elements for thermal and visible imaging in these bands. We show here that GLS glasses in which Ga_2Se_3 is introduced up to complete substitution of Ga_2S_3 by Ga_2Se_3 are suitable candidates for this role. Previous attempts to achieve this substitution were reported to be a failure as the GLS:Se glass had similar characteristics to that of a traditional GLS.[10] However, a deeper analysis of the quaternary system Ga-La-S-Se revealed the material to be very sensitive to the oxygen content. In principle, the substitution of sulphur with heavier chalcogens should produce phonons lower in frequency extending the transmission window of the glass.[11,12] Thus, an extended transmission window is expected theoretically and previous attempts to achieve this suffered from extrinsic impurities which masked the true potential at longer wavelengths. Equally important is the retention of UV–Visible transmission which was expected for low concentrations of Se.

The characteristic temperatures of the modified samples are expected to be lower than the original GLS as Ga_2Se_3 has a lower melting point than Ga_2S_3.[13] The thermal properties of the samples were studied also in correlation with the content of Se. In particular, the difference between the glass transition temperature and the crystallization temperature is investigated as in similar studies.[10,14,15]

The improvement arising from the Se-doping of GLS is now addressed to give a new perspective to the well-studied GLS glasses and to opening new horizons in the application of the materials in optics and photonics. The improved transmission window may be exploited in multispectral imaging producing lenses and other optical parts. The strong thermal and mechanical properties of Se-doped GLS can suit the production of those optical elements. The manufacturing of optical fibres can also be of interest for IR power delivery and fibre lasers.

Precursor mixtures of La_2S_3, Ga_2S_3 and Ga_2Se_3 were batched in a dry-nitrogen purged glove box and homogenized with the aid of a roller mixer for 1 h. The mixtures were melted in a vitreous

Table 1. Samples composition, characteristic temperatures, and coefficients of thermal expansion (CTE).

Sample number	Ga_2S_3 [mol%]	La_2S_3 [mol%]	Ga_2Se_3 [mol%]	T_g [°C]	T_x [°C]	T_m [°C]	K_W	CTE [$°C^{-1}$]
1[a)]	50	30	20	512	674	788	0.206	9.94×10^{-6}
2[a)]	40	30	30	516	661	785	0.185	9.92×10^{-6}
3[a)]	35	30	35	505	654	775	0.192	1.04×10^{-5}
4[a)]	30	30	40	500	655	773	0.201	1.06×10^{-5}
5[a)]	25	30	45	496	649	773	0.198	–
6[a)]	20	30	50	494	634	769	0.182	9.78×10^{-6}
7[a)]	15	30	55	496	633	768	0.178	–
8[a)]	10	30	60	497	627	767	0.169	9.56×10^{-6}
9[b,d)]	0	30	70	466	602	766	0.178	–
10[b)]	40	40	20	540	658	790	0.149	7.72×10^{-6}
11[b)]	45	35	20	538	664	789	0.160	1.29×10^{-5}
12[c)]	50	20	30	320 513	556 747	780	–	–
13[b)]	30	40	30	534	648	779	0.146	1.060×10^{-5}

[a)]Glassy phase; [b)]Glassy with particles; [c)]Spinodal decomposition; [d)]Melted with RF furnace.

carbon crucible and placed in an argon-purged silica tube. A horizontal tube furnace was used to produce Ga_2Se_3-doped GLS glasses with a melt-quench method. The average loss in mass around 2% mainly consisted of volatile oxides of sulphur and selenium. Glassy samples were cut into rectangular flats and polished with a mechanical–chemical process to produce samples suitable for optical characterization. The composition and the phase of the samples fabricated is summarized in **Table 1**. The phase classification was done initially by visual inspection and then confirmed with Raman spectroscopy. The spectra of crystalline samples are expected to exhibit sharp peaks within the range where the wide peak of amorphous compounds was found.[16]

Figure 1 is a sketch of the phase diagram for the system La_2S_3-Ga_2Se_3-Ga_2S_3. Based on previous studies on GLS glasses, the composition 70 mol% Ga_2S_3:30 mol% La_2S_3 was initially studied.

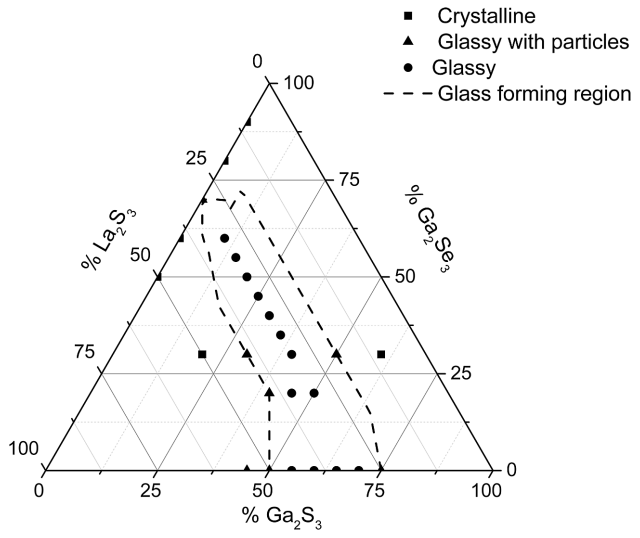

Figure 1. Phase diagram and glass forming region of the ternary system Ga_2S_3-Ga_2Se_3-La_2S_3.

It is the glass forming composition containing the largest quantity of Ga_2S_3 when oxide impurities are minimized, thereby allowing the highest possible substitution of sulphur for selenium.[17] In addition, Ga_2Se_3 could flux into Ga_2S_3 and avoid the partial or complete insolubility of La_2S_3 in the selenide compound.

The accuracy of these assumptions was confirmed as almost all the samples containing 70 mol% Ga_2Ch_3 (Ch = S,Se):30 mol% La_2S_3 formed a homogenous glass without indications of crystallization or phase separation (Samples 1–8).

For samples produced with a different Ga_2Ch_3(Ch = S,Se):La_2S_3 ratio, only Sample 11 produced crystals or glasses with particles again supporting the hypothesis about the highest chemical flexibility of the 70 mol% Ga_2Ch_3 (Ch = S,Se):30 mol% La_2S_3 composition.

For the production of Sample 9 (70 mol% Ga_2Se_3:30 mol% La_2S_3), the quenching conditions which produced glasses in previous samples did not result in an amorphous solid. It was thought that the complete substitution of Ga_2S_3 by Ga_2Se_3 may require higher quenching rates. Quenching rates were increased using a RF furnace which selectively heated up only the vitreous carbon crucible containing the mixture. As a result, the system experienced a larger heat exchange with the surrounding atmosphere and the quenching step occurred at a faster cooling rate. The improved quenching condition allowed Sample 9 to be produced with an amorphous. This observation is consistent with similar studies where higher cooling rates are necessary when amorphous As_2S_3 is gradually added modified with increasing amounts of Se and Te.[18]

Figure 1 also reports the glass-forming region of the ternary system La_2S_3-Ga_2Se_3-Ga_2S_3 with reference to the phase of the samples (Table 1). It cannot be excluded that variations in the fabrication process can alter the glass-forming region. For example, as demonstrated with Sample 9, a faster quenching from the melt may produce homogenous glasses where the present study indicated crystalline compositions.

Figure 2 (bottom) shows the Raman spectra of two samples with composition 70 mol% Ga_2Ch_3 (Ch = S, Se):30 mol% La_2S_3.

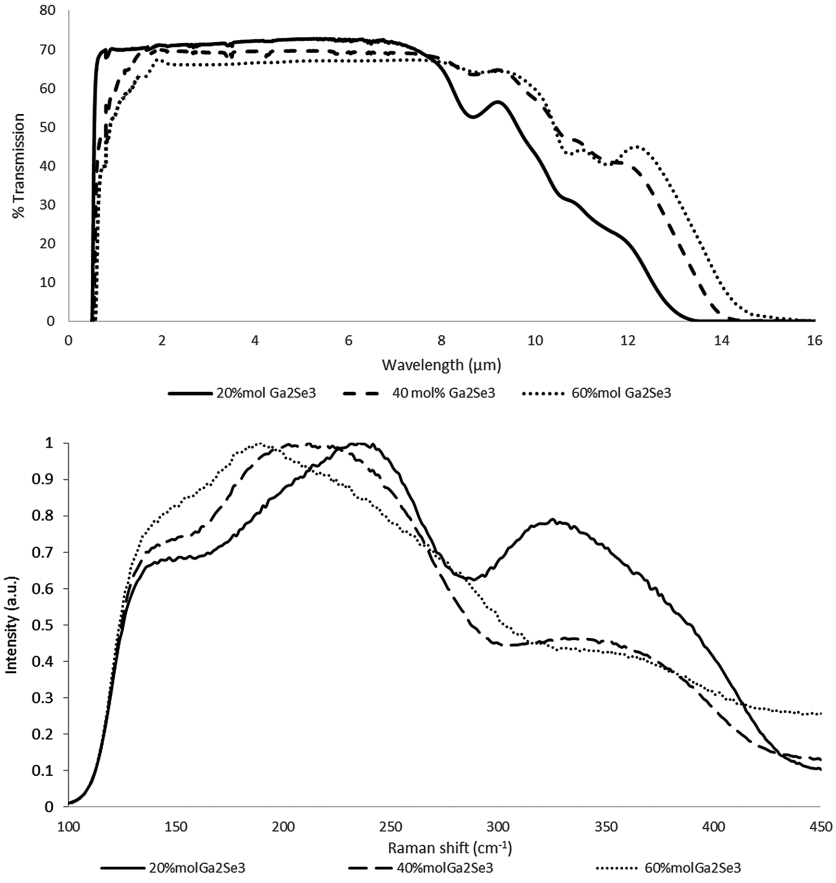

Figure 2. Transmission window (top) and Raman spectra (bottom) of samples 1 and 8. For clarity, data about intermediate compositions have been omitted.

The plot includes spectra for samples containing 20, 40, and 60 mol% of Ga_2Se_3. The spectra of intermediate compositions were omitted for clarity. The peak centred at 325 cm^{-1} was assigned to the symmetric vibration of tetrahedral GaS_4 as the intensity of this feature gradually falls as the concentration of Ga_2S_3 decreases. In addition, GaS_4 has the highest frequency vibrations, which is consistent with light metal sulfides. Variations of the position of this peak may depend on the composition of the host as reported by previous studies.[19]

The second band centered at about 225 cm^{-1} corresponds to heavier elements or weakly bonded species. As the concentration of Ga_2Se_3 is increased the intensity of this band was also increased and moved toward less energetic vibrations. This observation is in good agreement with previous studies on selenide glasses with Raman features around 240 cm^{-1}. Thus, this peak may be assigned to $GaSe_4$ tetrahedra.[2] The other two features notably changed both position and intensity according with allocation to the sulfide species. As shown in Figure 2, the $GaSe_4$ peak shifts from 225 to 195 cm^{-1} as the concentration of the selenide species was increased. This observation can be explained as a structural rearrangement of the glass network in which Se contributes as a modifier at low concentration and as a network former at high concentrations.

Finally, the shoulder peaks around 150 cm^{-1} is a constant feature for all the spectra. Previous work on La_2S_3 reported several Raman-active modes around 150 cm^{-1} for this compound.[20] Therefore, this peak can be assigned to La_2S_3, the quantity of which is invariant in Samples 1 to 9.

Figure 2 (top) shows the absorption of samples with composition 70 mol% Ga_2Ch_3 (Ch = S, Se):30 mol% La_2S_3 in a range between 0.5 and 16 μm. As expected, the electronic edge moves toward the infrared resulting in a reduced bandgap as a result of the replacement of S for Se.[21] However, samples with a large amount of Ga_2Se_3 (e.g., Sample 8) retain some transmission in the visible range. This observation was unexpected as other substitutions for heavier elements (i.e., Ga for In) were reported to cause dramatic red shifts to the transmission window.[22]

On the other hand, for all samples modified with Se, the infrared cut-off is at significantly longer wavelengths than for GLS, where the absorption edge is at 9 μm.[17] Particularly, the edge moves from around 13 μm for Sample 2 to about 15 μm for Sample 8 and Sample 9. This substantial improvement of the infrared transmission is due to the addition of Se, which decreases the energy of the molecular vibrations placing the multiphonon edge at longer wavelengths, i.e., lower energies.

Thermal analysis was carried out as per the procedure described in the Experimental Section. Table 1 summarizes the results obtained for the glass transition temperature (T_g), onset of crystallization (T_x), melting temperature (T_m), and the calculated Weinberg parameter (K_W). The Weinberg parameter was used to estimate the thermal stability of the glasses. It was reported to be more accurate than the commonly used Hruby's parameter, hence the reason to report it.[2] The Weinberg parameter relates the $T_g - T_x$ gap with the T_m representing the overall stability of the samples. It is defined as[14]

$$K_W = \frac{T_x - T_g}{T_m} \quad (1)$$

Due to the lower melting point of Ga_2Se_3, all the samples exhibited lower characteristic temperatures than the original GLS glass.[10] The value of K_W for samples with composition 70 mol% Ga_2Ch_3 (Ch = S, Se):30 mol% La_2S_3 decreases as the weaker Ga—Se bonds replace Ga—S bonds. However, almost all the compositions are characterized by a better thermal stability than GLS glass as indicated by higher value of K_W for Se-added GLS.[17] A small change in the T_g was observed over the range of compositions from Sample 3 to Sample 6, while the complete substitution of Ga_2S_3 by Ga_2Se_3 brings more pronounced changes. This implies that Ga_2S_3 had the strongest effect on the chemistry of the original GLS at low and very high concentration. The largest reduction was observed for Sample 9 for which the T_g was 87 °C lower than the original GLS glass previously measured as high as 553 °C.[17]

The glass transition temperature was found to be largely changed for samples with a fixed concentration of Ga_2Se_3 as the amount of sulfides was varied. The highest change was observed between Sample 1 (50 mol% Ga_2S_3) and Sample 10 (40 mol% Ga_2S_3), for which the T_g decreased by 28 °C as the amount of Ga_2S_3 was increased. This observation can be accounted with the formation of stronger covalent bonds belonging to La_2S_3 leading to a higher T_g.

The thermal analysis of Sample 12 revealed two glass transition temperatures for this composition. This observation was reported for glasses undergoing phase separation in the melt or spinodal decomposition.[23,24] The formation of multiple glassy phases results in the transmission significantly decreased due to scattering from refractive index variations between the two phases. The phase with low T_g and T_x (330 and 556 °C, respectively) could be characterized as a composition with a low concentration of La and high concentration of Se. On the other hand, the phase with high T_g and T_x (513 and 747 °C, respectively) shows thermal features similar to Sample 1 which may indicate a concentration of Se around 20 mol%.

As shown in Table 1, a number of samples possess multiple crystallization peaks. This agrees with previous works on crystallized GLS glasses for which two possible crystal phases were recognized. The peaks may be overlapped in the plots of samples with only one crystallization peak.[25]

The viscosity curves were investigated for samples with composition 70 mol% Ga_2Ch_3(Ch = S,Se):30 mol% La_2S_3 following the equation reported in the method ISO 7887-4

$$\eta = 681 \cdot \frac{l_s^3 \Delta t m}{I_c \Delta f} \tag{2}$$

η is the viscosity (dPa s), l_s is the span of the three point bending stage (mm), Δt is the measured time (s), m is the load applied on the sample in (g), I_c is the cross-sectional moment of inertia in (mm^4), and Δf is the change in position of the probe measured (mm).

The curves were subsequently fitted to the Vogel–Fulcher–Tammann equation in the form

$$\log(\eta) = k + \frac{a}{T - b} \tag{3}$$

where T is the temperature of the sample, k, a, and b are constants.[26] The least square method was used for this fitting. The curve was plotted from 480 to 690 °C in order to have a projection of the behaviour of the materials over a larger range of temperatures.

Figure 3 shows the fitted curves in a range between 480 and 690 °C. When the T_g of each respective materials was reached the fittings gave values of viscosity around 10^{13} dPa s proving the accuracy of the measurements. The softening point defined as $T_\eta = 10^{7.6}$ spanned from 564 to 623 °C over the range of compositions. As expected, the incremental addition of Ga_2Se_3 shifted the curves toward lower values of viscosity within the range. This effect was due to the formation of weaker metal–selenium bonds. However, the viscosity of Sample 4 was found to be higher than Sample 2 despite the higher concentration of selenium.

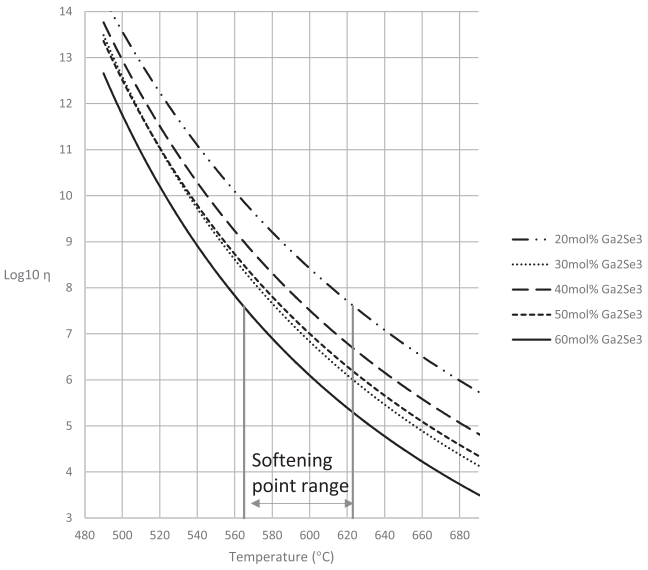

Figure 3. Viscosity curves for samples 1, 2, 4, 6, 8.

The same trend was observed for K_W and coefficient of thermal expansion (CTE) (Table 1). The occurrence of this bell-shaped trend centered on 40 mol% Ga_2Se_3 can be due to the nature of the bonding that builds the glassy network. In particular, Ga—S and Ga—Se bonds are of a covalent type, while La—S bond is a strong bond having more ionic character. Since Ga—Ch bonds (Ch = S,Se) are predominant in the materials, the thermal expansion coefficients were found to be close to what reported for other chalcogenides.[3,27] The initial decrease of the values of CTE, viscosity, and K_W for low concentration of selenium may be due to the transition from La—S to much weaker La—Se bonds. Subsequently, for a concentration of 40 mol% Ga_2Se_3 peak values of CTE and K_W and stable viscosity may be observed as a result of the formation of Se—S bonds which are stronger than Ga—S and Ga—Se bonds and therefore more likely to be formed. However, the CTE measured for all the samples was higher than the original GLS glass indicating a strong contribution of metal–selenium bonds to the CTE.[17]

In conclusion, the modification of GLS with Ga_2Se_3 resulted in a novel material with promising feature for many applications in optics and photonics. The improved optical and thermomechanical characteristics make this glass a promising material for active and passive applications. In particular, the large transmission window can enable new approache in combining thermal and visible imaging. In addition, the possibility to tailor refractive index with appropriate content of Se can be used for new chalcogenide optical fibres and graded index lenses.

Experimental Section

The samples were prepared following the procedure described above. The batches were baked at 350 °C for 3 h to eliminate volatile compounds and then melted at 1150 °C for 24 h. A ramp rate of 10 °C min^{-1} was used in both stages. The tube was purged with dry argon at a flow rate of 500 sccm. The samples were annealed at 490 °C for 24 h at a ramp rate of 1 °C min^{-1}. The Raman spectra were measured with a Renishaw

"inVia" Raman spectrometer equipped with a laser with $\lambda = 532$ nm. The transmission window of samples with thickness around 1mm was measured using a nitrogen-purged Varian 670-IR FTIR spectrometer and Cary 50 UV-Vis spectrophotometer scanning over a range of wavelengths between 6000 and 500 cm^{-1}.

Grains of around 10 mg in weight were used to determine the glass transition temperature (T_g), onset crystallization (T_x), and melting temperature (T_m) with the aid of a Perkin-Elmer Diamond TG-DTA. The viscosity and the coefficient of thermal expansion (CTE) were measured with a thermal mechanical analyser (Perkin-Elmer Diamond TMA). For the viscosity curves, slabs of 1 mm in thickness and edges of 1 mm × 5 mm in length. For the CTE, a squared rod of 1 cm in height and edges 1 mm × 1 mm in length were used.

Acknowledgements

This work was funded by the Engineering and Physical Sciences Research Council (EPSRC) grant EP/M015130/1 for ChAMP, the Chalcogenide Advanced Manufacturing Programme. The authors have no underpinning data that needed archival storage within the content of this work.

Conflict of Interest

The authors declare no conflict of interest.

Keywords

amorphous materials, chalcogenides, gallium lanthanum sulfide glass

Received: November 22, 2016
Revised: March 21, 2017
Published online:

[1] B. J. Eggleton, B. Luther-Davies, R. Kathleen, *Nat. Photonics* **2011**, *5*, 725.
[2] J. S. Sanghera, I. D. Aggarwal, *Infrared Fibre Optics*, 1st ed., CRC Press, Washington, DC, USA **1998**.
[3] A. B. Seddon, *J. Non-Cryst. Solids* **1995**, *184*, 44.
[4] A. Zakery, S. Elliott, *J. Non-Cryst. Solids* **2003**, *330*, 1.
[5] M. Hughes, H. Rutt, D. Hewak, R. J. Curry, *Appl. Phys. Lett.* **2007**, *90*, 3.
[6] M. A. Hughes, J. E. Aronson, W. S. Brocklesby, D. P. Shepherd, D. W. Hewak, R. J. Curry, *Proc. SPIE* **2004**, *5620*, 289.
[7] M. A. Hughes, R. J. Curry, D. W. Hewak, *J. Opt. Soc. Am. B* **2008**, *25*, 1458.
[8] T. Schweizer, D. W. Hewak, B. N. Samson, D. N. Payne, *J. Lumin.* **1997**, *72–74*, 419.
[9] T. Schweizer, D. Brady, D. W. Hewak, *Opt. Express* **1997**, *1*, 102.
[10] J. D. Shephard, R. I. Kangley, R. J. Hand, D. Furniss, M. O'Donnell, C. A. Miller, A. B. Seddon, *J. Non-Cryst. Solids* **2003**, *326*, 439.
[11] S. Shabahang, G. Tao, J. J. Kaufman, A. F. Abouraddy, *J. Opt. Soc. Am. B* **2013**, *30*, 2498.
[12] A. B. Seddon, Z. Tang, D. Furniss, S. Sujecki, T. M. Benson, *Opt. Express* **2010**, *18*, 26704.
[13] D. L. Perry, in *Handbook of Inorganic Compounds*, CRC Press, Boca Raton, FL, USA **2011**, p. 84.
[14] A. F. Kozmidis-Petrovi, *Thermochim. Acta* **2010**, *499*, 54.
[15] J. D. Shephard, R. I. Kangley, R. J. Hand, D. Furniss, C. A. Miller, A. B. Seddon, *J. Non-Cryst. Solids* **2003**, *332*, 271.
[16] J. R. Ferraro, K. Nakamoto, C. W. Brown, *Introductory Raman Spectroscopy*, Academic Press, San Diego, CA, USA **2003**.
[17] P. Bastock, C. Craig, K. Khan, E. Weatherby, J. Yao, D. W. Hewak, CLEO 2015, IEEE, San Jose, CA, USA **2015**.
[18] V. S. Shiryaev, M. F. Churbanov, *Chalcogenide Glasses*, Woodhead Publishing, Cambridge, UK **2014**, p. 3.
[19] C. Julien, S. Barnier, M. Massot, N. Chbani, X. Cai, A. M. Loireau-Lozac'h, M. Guittard, *Mater. Sci. Eng. B* **1994**, *22*, 191.
[20] M. Dunleavy, G. C. Allen, M. Paul, *Adv. Mater.* **1992**, *4*, 424.
[21] I. D. Aggarwal, J. S. Sanghera, *J. Optoelectron. Adv. Mater.* **2002**, *4*, 665.
[22] T. Schweizer, D. J. Brady, D. W. Hewak, Y. D. West, *Fiber Integr. Opt.* **2000**, *19*, 229.
[23] P. Gabbot, *Principles, Applications of Thermal Analysis*, Wiley-Blackwell, Oxford, UK **2008**.
[24] E. P. Fel, L. I. Stefanovich, *Sov. Phys. JEPT*, **1991**, *1704*, 951.
[25] R. Li, A. B. Seddon, *J. Non-Cryst. Solids* **1999**, *257*, 17.
[26] C. Vitale-Brovarone, G. Novajra, J. Lousteau, D. Milanese, S. Raimondo, M. Fornaro, *Acta Biomater.* **2012**, *8*, 1125.
[27] F. A. S. Al-Alamy, A. A. Balchin, M. White, *J. Mater. Sci.* **1977**, *12*, 2037.